Acute Leukemia Subtype Recognition in Blood Smear Images with Machine Learning

Original Scientific Paper

Ashwini P. Patil*

Department of Computer Science, CHRIST (Deemed to be University),
Bengaluru, India
patil.ashwini.p@gmail.com

Manjunatha Hiremath

Department of Computer Science, CHRIST (Deemed to be University),
Bengaluru, India
manju.gmtl@gmail.com

*Corresponding author

Abstract – Acute leukemia is a swiftly progressing blood cancer affecting white blood cells which poses a significant threat to the immune system and often leads to fatal outcomes if not detected and treated promptly. The current manual diagnostic method, being time-consuming and prone to errors, necessitates an urgent shift toward a comprehensive automated system. This paper presents an innovative approach to automatically identify acute leukemia cells and their subtypes by analyzing microscopic blood smear images. The proposed methodology involves the segmentation of clustered lymphocytes, isolation of nuclei, and extraction of diverse features from each nucleus. A random forest classifier is then trained to categorize nuclei into healthy or cancerous, with further precision in classifying cancerous nuclei into specific subtypes. The method achieves an impressive 97% accuracy across all evaluations, holding profound implications for pathologists and medical practitioners in their decision-making processes

1. INTRODUCTION

Leukemia is anticipated to witness a 35.1% surge in cases across Asia between 2020 and 2040, as projected by the World Health Organization's International Agency for Research on Cancer [1]. This cancer targets white blood cells, integral to our immune system. It triggers the excessive production of abnormal white blood cells within the blood and bone marrow, potentially spreading to other organs and compromising immunity. The disease is broadly classified into four main types: Acute Lymphoblastic Leukemia (ALL), Acute Myeloid Leukemia (AML), Chronic Lymphocytic Leukemia (CLL), and Chronic Myeloid Leukemia (CML). The classification of leukemia depends on its progression speed and affected cell lineage. Acute leukemia, with its swift progression, features immature blasts multiplying rapidly in the bone marrow, causing sudden symptoms. In contrast, chronic leukemia advances more slowly, with mature abnormal cells resembling normal ones, resulting in a gradual onset of symptoms. Lymphoid or myeloid categorization depends on the origin of affected white blood cells.

According to FAB classification within each primary category multiple subtypes exist. The subtypes of Acute Lymphoblastic Leukemia (ALL) are categorized as L1, L2, and L3. L1 is characterized by small and uniform lymphoblasts while L2 involves larger and more diverse lymphoblasts. L3 also identified as Burkitt's leukemia is distinguished by large lymphoblasts with intense staining. The classification of Acute Myeloid Leukemia (AML) spans from M0 to M7. M0 denotes undifferentiated AML with undefined characteristics, while M1 through M5 signify increasingly mature myeloid cells. M6 signifies acute erythroleukemia, involving both erythroid and myeloid precursors, and M7 is linked to acute megakaryoblastic leukemia, characterized by abnormal megakaryocytes.

Advancements in genetic research have significantly enhanced our understanding of leukemia, leading to ongoing changes in classification systems, such as the World Health Organization's (WHO) classification. The complexity of leukemia arises from a combination of genetic, molecular, and cytogenetic factors, making each case unique [2, 3]. Factors like leukemia type, age,

overall health, genetics, and exposure to risk elements contribute to varying risks associated with the disease.

Current manual diagnosis methods, involving the analysis of blood smears and bone marrow smears under a microscope, have limitations due to subjective interpretations and lack of quantitative precision, particularly in distinguishing visually similar leukemia subtypes. In response to these challenges, machine learning has emerged as a promising solution for leukemia diagnosis [4]. Utilizing sophisticated algorithms, machine learning provides a quantitative assessment of cell morphology, detects intricate patterns, and objectively evaluates anomalies, reducing human subjectivity. In summary, machine learning revolutionizes our approach to leukemia, promising improved patient care and enriching research insights by elevating accuracy and adapting to evolving disease characteristics.

The focal point of this research paper is the utilization of machine learning methodologies for the detection and classification of the main types and subtypes of acute leukemia. This model stands poised to assist pathologists and medical practitioners in decision-making processes. The paper's structure unfolds as follows: Section 1 presents the study's scope; Section 2 delves into the realm of literature review; Section 3 furnishes dataset particulars; Section 4 elaborates on the proposed methodology; Section 5 discusses experimental outcomes; and Section 6 culminates in a conclusive wrap-up.

2. BACKGROUND AND RELATED WORKS

The critical nature of leukemia necessitates early diagnosis for effective treatment. To achieve this, various automated systems have been developed, leveraging affordable microscopic image analysis, to facilitate timely and accurate diagnoses. Putzu et al. [5] introduced a fully automated method for Acute Lymphoblastic Leukemia (ALL) classification achieving 93% accuracy using SVM-based machine learning on the ALL-IDB database. Mohapatra et al. [6] achieved a notable 99% classification accuracy with an ensemble-based technique on their private dataset. Rawat et al. [7] distinguished acute lymphoblast and acute myeloblast subtypes, attaining an exceptional 99.5% overall accuracy with a publicly available dataset.

Inbarani et al. [8] applied an innovative hybrid histogram-based soft covering rough k-means clustering (HSCRKM) algorithm for segmenting leukemia nucleus images. Devi et al.[9] introduced an innovative approach incorporating Gaussian Blurring, Hue Saturation Value (HSV) and morphological operations, achieving 96.30% accuracy using private dataset whereas 95.41% using ALL-IDB1 public dataset. M. Ashok et al. [10] proposed an automated machine learning approach (Chabot) achieving accurate classification of infected and healthy cells in blood smear images, aiming to detect ALL by utilizing CMYK color space and K-means clustering.

While interpretable and resource-efficient, traditional machine learning models may fall short in capturing intricate patterns within medical images compared to the effectiveness of deep learning, particularly transfer learning, known for its high accuracy in leukemia detection and classification [11, 12]. Ansari et al. [13] suggested CNN model which uses Tversky loss function, designed for the classification of acute leukemia images, attained an impressive accuracy rate of 99%. Boldú et al. [14] constructed with two sequentially connected convolutional networks (ALNET), was trained using a dataset comprising over 16,000 blood cell images collected from clinical practice. Abass et al. [15] proposed CAD3 system utilizing YOLO v2 and CNN for leukocyte detection and classification.

One of the challenges in deep learning is the availability of large datasets, and in many cases, these datasets may not be properly labeled [16]. Manescu et al. [17] used patient diagnostic labels to train weakly-supervised models for the detection of various acute leukemia types. Depto et al. [18] explore various deep learning approaches designed to address imbalanced classification issues. AI techniques were used to assess the interpretability of these often considered "black box" models [19].

Certain researchers leverage the advantages of both machine learning and deep learning. They often use deep techniques for feature extraction and traditional algorithms for tasks like segmentation and classification. Elhassan et al. [20] utilized CMYK-moment localization and CNN-based feature extraction, while, Jha et al. [21] integrated segmentation from active contour and fuzzy C means, employing a Chronological SCA-based Deep CNN classifier for classification.

3. DATA DESCRIPTION

Publicly available blood smear datasets offer a valuable resource for investigating a range of blood-related disorders, like anemia, infections, and leukemia. Such datasets are instrumental in the development and validation of automated image analysis algorithms, machine learning models, and computer-aided diagnostic tools. This advancement enhances the precision and efficiency of blood smear examination and holds the potential to transform the field of hematological disease detection and classification. Additionally, these public datasets foster collaboration among researchers, encourage the establishment of standardized protocols, and facilitate the evaluation of various methodologies. As a result, patient care and diagnostic accuracy stand to benefit substantially from these collective efforts

This research utilizes the Raabin Health dataset [22], comprising 40,000 microscopic smears of WBCs from blood samples collected from patients who visited the Raabin collaborator medical laboratory in Tehran. The images are stained using the Giemsa technique and captured with a Zeiss microscope with a 100x zoom capac-

ity and LG G3 Smartphone. In this research a total of 800 blood smear images representing ALL, AML, and healthy samples have been included. Nuclei are automatically extracted from each image generating sub images. The dataset is split into 20% for testing and 80% for training. The distribution of images for each classification label is provided in Table 1, while Fig.1. illustrates sample leukemia images extracted from the database

Table 1. Distribution of Images

Type	Sub Types	Images	Nucleus sub images
Acute Lymphoblastic Leukemia (ALL)	L1	100	217
	L2	100	519
Acute Myeloid Leukemia (AML)	M0	100	234
	M1	100	204
	M3	100	307
	M4	100	339
	M5	100	495
Healthy	Healthy	100	100
Total	M6	800	2415
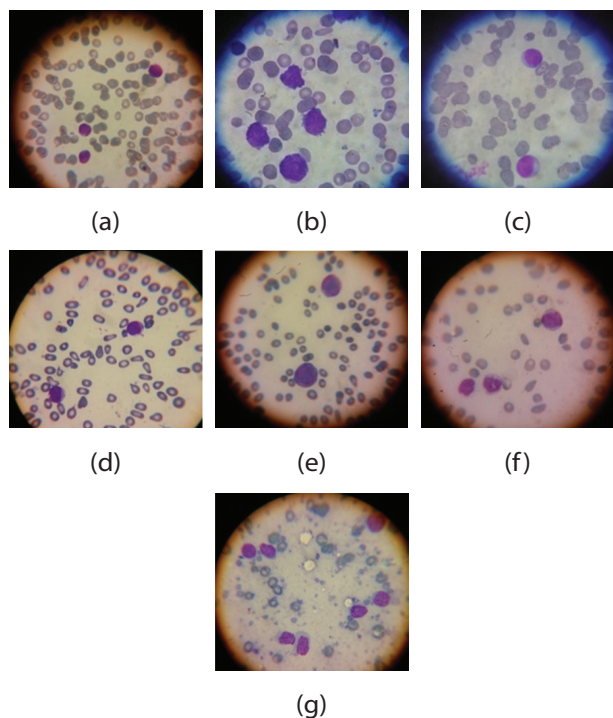
Fig. 1. Sample images from dataset (**a**) ALL-L1; (**b**) ALL-L2; (**c**) AML-M0; (**d**) AML-M1; (**e**)AML-M2; (**f**)AML-M3; (**g**) and AML-M5

4. PROPOSED WORK

4.1. SEGMENTATION AND NUCLEUS CROPPING

In medical image processing, resizing images is a standard preprocessing procedure aimed at ensuring uniformity in analysis and facilitating consistent feature extraction across diverse images, allowing for effective feature comparison. Hence, resizing operations are employed across all images to standardize their dimensions. The region of interest of our research is white blood cells, which need to be segmented from blood smear images. Initially, the procedure involves isolating the green channel data from the original RGB image because nucleus is more evident in the green channel [5].

A new image is created, preserving the original green channel data while substituting the red and blue channels with zeros, thereby retaining only the green channel's information. Median filter is applied to green channel image to reduce noise and improve quality of the image (see Fig 2). Subsequently, this newly formed image is converted from the YCbCr color space to the RGB color space. This transformation renders an image where the luminance data from the green channel is retained while lacking the color data from the chrominance (Cb and Cr) channels.
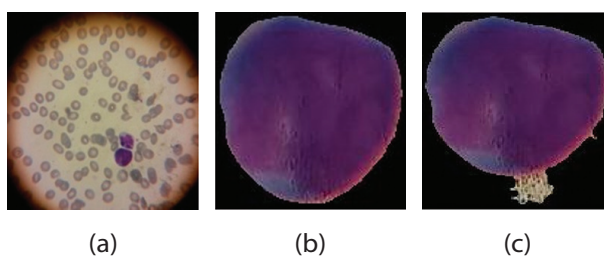
Fig. 2. Median Filter (**a**) Original Image; (**b**) With median filter; (**c**) Without median filter

To enhance contrast of the image, it is converted to grayscale and a histogram equalization technique is applied. The next step involves converting the image to a binary format using gray thresholding, which isolates the white blood cells while eliminating background elements like red blood cells and platelets. If white blood cells are connected or in proximity, further segmentation is necessary to differentiate them. The process includes employing the canny edge detection algorithm on the binary image to highlight edges. Morphological operations such as dilation are performed to enlarge the white regions, aiding in connecting fragmented edges and improving features. Filling operations are carried out to complete or bridge gaps in white regions, followed by erosion to decrease white region size, potentially separating interconnected regions and eliminating smaller objects.

A distance transform is calculated, and watershed segmentation is applied to segregate linked cells. The outcome of watershed segmentation undergoes a refinement process where undesired small objects are eliminated from a binary image. This is achieved by considering their area size, and the resulting refined output serves as a mask. This mask is then utilized to apply the Bounding Box technique for precisely extracting each nucleus from blood smear images. This comprehensive sequence of procedures enables effective identification and separation of white blood cells into sub-images. The results at all stages are collectively visualized in Fig 3 and fundamental stages of sub-image creation are outlined in Algorithm 1 as follows.

Algorithm 1

Input: Microscopic Blood smear images

Output: Nucleus sub image

1 Let $I_{resized}(x, y)$ represents the image $I(x, y)$ after resizing to a standard size

2 $G(x, y) = I_{resized}(x, y)\ green$
Where, $G(x, y)$ is isolated green channel

3 Convert the $E(x, y)$ to image while preserving green channel
$E(x, y) = \begin{cases} E(x, y) \\ 0 \end{cases}$

4 Noise reduction with median filter
$E(x, y) = Median\ E(x, y), [m, n]$
Where, $[m, n]$ defines median filter size 3×3

5 $J(x, y) = RGB(E(x, y))$
Where, $RGB(E(x, y))$ signifies transformation of $E(x, y)$ from YCbCr color space to RGB color space

6 Convert the RGB image $J(x, y)$ to grayscale image
$K(x, y) = grayscale(J(x, y))$

7 Apply histogram equalization to $K(x, y)$

8 $B(x, y) - Binary(K(x, y), T)$
Where, $Binary(K(x, y), T)$ applies binary transformation to each pixel in the grayscale image $K(x, y)$ using threshold value T

9 Edge detection using canny edge detector
$C(x, y) = edge(B(x, y), 'Canny')$

10 Performing morphological operation including dilation, hole filling, and erosion on $C(x, y)$
$R(x, y) \rightarrow Morphological\ operations(C(x, y))$

11 $T(x, y) = Distance\ Transform(R(x, y))$
$S(x, y) = watershed(T(x, y))$
Where $R(x, y)$ is binary image after morphological operation,
And $T(x, y)$ represent distance transform image,
$S(x, y)$ is segmented image obtain by applying watershed segmentation algorithm

12 $M = Removesmallobjects(I, min\_area)$
Where M is the refined binary image used as a mask to indicate region of interest

13 Boundary box is applied using generated mask M
$Nuclei = BoundingBox(I, M)$
Where I is original image
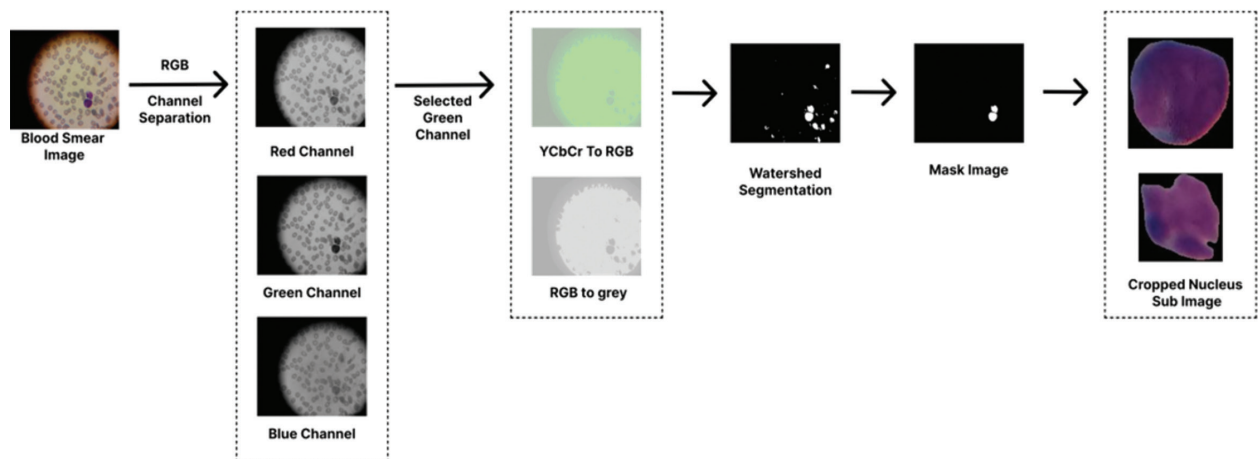
Fig. 3. White blood cell (WBC) segmentation and cropping

Tabel 2. List of features

	Feature Method	Extracted Feature
Texture Features	Gray-Level Co-occurrence Matrix (GLCM)	Contrast, Correlation, Energy, Entropy, Homogeneity, Sum of squares, Sum average, Sum variance, Sum entropy, Difference variance, Difference entropy, Information measure of correlation1, Informaiton measure of correlation2
	Local Binary Pattern (LBP)	LBP values for the histogram bins
Geometrical Features		Area, Perimeter, EquivDiameter, EulerNumber, MajorAxisLength, MinorAxisLength, Solidity, Eccentricity, Circularity, ConvexArea, Extent
Color Features	Color Moments features in LAB color space	mean, Standard Deviation of Color Channels, skewness, kurtosis
Statistical Features	Higher-Order Statistical Moments	Skewness, Kurtosis

4.2. FEATURE EXTRACTION

In medical image processing feature extraction is crucial for condensing intricate pixel data into a meaningful representation of patterns, textures, and ana-tomical structures. This research considers 48 features as listed in Table 2 extracted from nucleus sub-images contributing to leukemia detection from blood smear images. Subtypes of AML and ALL are identified based on morphological features. Shape, size and chromatic

pattern of nucleus vary for different subtypes. Some cells appear primitive while few cells show more mature cell features. Texture features, specifically Local Binary Pattern (LBP) and Gray-Level Co-occurrence Matrix (GLCM), amplify the effectiveness of leukemia detection from blood smear images. LBP excels in capturing intricate local texture patterns by comparing pixel intensity variations, while GLCM comprehensively analyzes spatial relationships between intensity values. Geometrical features provide quantitative insights into cell shape, size, and arrangement, incorporating parameters such as cell area, perimeter, circularity, and eccentricity, thus presenting a comprehensive depiction of cell morphology.

Color Moments features extracted from the LAB color space, significantly contribute to leukemia detection. LAB color space's separation of luminance (L) from chromatic information enhances robustness to lighting variations. These Color Moments, including mean, standard deviation, and skewness, effectively capture color distribution characteristics, thereby highlighting variations in cell staining and aiding the differentiation of normal and leukemia-affected cells. Moreover, higher-order statistical moments encompassing skewness and kurtosis go beyond mean and variance, revealing complex statistical patterns. These moments provide insights into distribution asymmetry and peakedness, uncovering subtle textural irregularities indicative of abnormal cell structures. By quantifying non-uniformities and deviations from a standard distribution, higher-order statistical moments further enhance the ability to differentiate between normal and leukemia-affected cells.

All the extracted features are normalized to ensure they are on similar scale to improve efficiency of classification algorithm and reduce the effect of features with large numerical values dominating the learning process. After features are extracted and normalized they are concatenated into a single feature vector. This feature vector contains unique characteristics of each image in a compact format. This diverse feature integration significantly enhances the precision and sensitivity of automated disease detection systems.

4.3. CLASSIFICATION

The utilization of the Random Forest algorithm presents a potent approach for the detection of leukemia from blood smear images. This algorithm, characterized by an ensemble of decision trees, is adept at handling the intricacies of medical image analysis. Random Forest algorithm can be formulated as:

$$Y_{prediction} = \arg\max_j \sum_{i=1}^{N_{trees}} I(y_i = j) \qquad (1)$$

Where: $Y_{prediction}$ is the predicted class for the sample, N_{trees} is the number of decision trees in the Random Forest. Y_i, j is the predicted class of the i-th decision tree for class j. $I(.)$ is the indicator function that returns 1 if the condition is true and 0 otherwise.
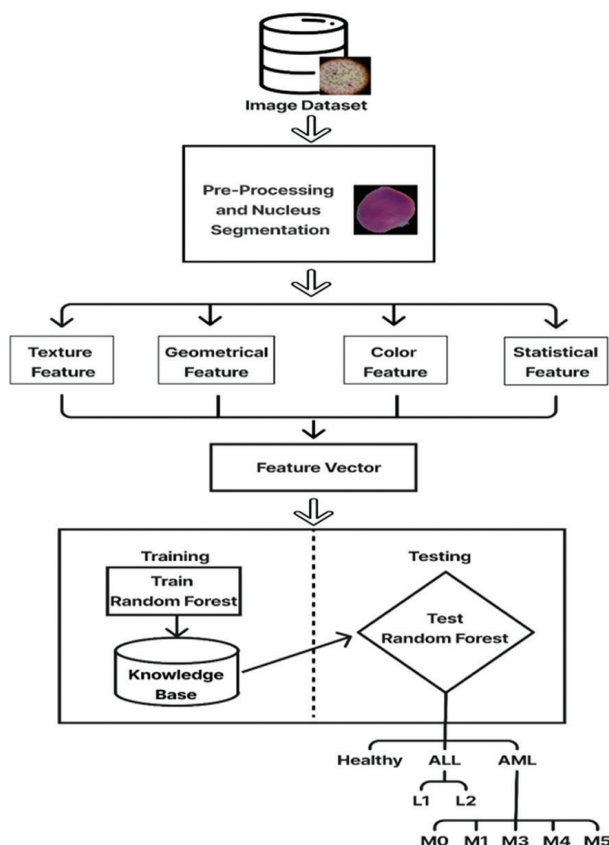
Fig. 4. Automated classification system for Acute leukemia

By employing features extracted from the images, such as texture features like GLCM and LBP, geometrical attributes, and Color Moments from the LAB color space, the algorithm can learn intricate patterns associated with normal and leukemia affected cells. The feature vector created by concatenating 48 features is given as an input for the classifier. Each feature is significant in capturing distinct aspects of cell morphology crucial for subtype classification in leukemia. All features are weighted equally in the classification process, reflecting their collective importance in discerning subtle variations indicative of different leukemia types and subtypes. The Random Forest model is trained on these features, and its collective decision-making process, combining outputs from individual trees, enables accurate classification. Through evaluation metrics like recall, precision, and F1-score, the effectiveness of the model is estimated, offering a robust and efficient tool for automated leukemia detection

5. EXPERIMENTAL RESULTS AND DISCUSSION

The comprehensive approach outlined for the detection of acute leukemia, including its types and subtypes, is visually represented in Fig 4. The focus of the proposed research is on multi-label classification, specifically involving the categorization of blood smear images into two main classes: healthy and cancerous. Within the cancerous category, a further distinction is made among different acute leukemia types and subtypes.

The effectiveness of the model is gauged through different performance parameters such as accuracy, precision, recall, and the F1 score. These results are presented in Table 3. For the experimentation, a dataset comprising 2415 nucleus sub-images is employed. To ensure robust evaluation, 20% of these images (483 in total) are designated for testing, while the remaining 80% constitute the training dataset. Among the testing nucleus images, 451 are successfully assigned to their respective categories. Notably, due to the presence of images with varying sizes for each label within the testing dataset, the consideration of the F1 score is crucial to accurately assess the model's performance.

Tabel 3. Performance measure

	Precision	Recall	F1-Score	Support
HL	0.93	0.87	0.90	15
L1	0.98	0.94	0.96	51
L2	1.00	1.00	1.00	103
M0	1.00	0.98	0.99	44
M1	1.00	0.98	0.99	41
M3	1.00	0.89	0.94	63
M4	0.88	0.99	0.93	70
M5	0.95	0.99	0.97	96
Accuracy			0.97	483
macro avg	0.97	0.95	0.96	483
weighted avg	0.97	0.97	0.97	483

The F1 score, a metric that harmonizes precision and recall, becomes particularly valuable when dealing with datasets characterized by imbalanced class distributions. This is a common scenario where one class vastly outweighs the other. Notably, the F1 score is calculated by balancing the trade-off between precision and recall. In this research, the F1 scores exhibit notable variation across the different categories. Specifically, healthy cells achieve an F1 score of 90%, while L1 and L2 types achieve 96% and 100%, respectively. Similarly, M0 and M1 categories have F1 scores of 99%, whereas M3, M4, and M5 exhibit scores of 94%, 93%, and 97%, respectively. In totality, the model achieves an overall accuracy of 97%. A comprehensive understanding of the model's performance, encompassing correctly classified instances, false positives, and false negatives, is provided through the confusion matrix (refer to Fig. 5(a)).

The ROC curve is created by plotting the True Positive Rate (TPR) on the vertical axis and the False Positive Rate (FPR) on the horizontal axis, while varying the threshold values (refer to Fig. 5(b)). Every point on the ROC curve corresponds to a specific threshold setting. The primary purpose of the ROC curve lies in evaluating the balance between sensitivity (true positive rate) and specificity (true negative rate) across different threshold choices. In addition to the curve itself, the Area Under the ROC Curve (AUC-ROC) is a widely utilized summary metric. The AUC-ROC value serves as an extensive assessment of the model's performance in distinguishing between classes, regardless of the specific threshold employed.

(a)

(b)
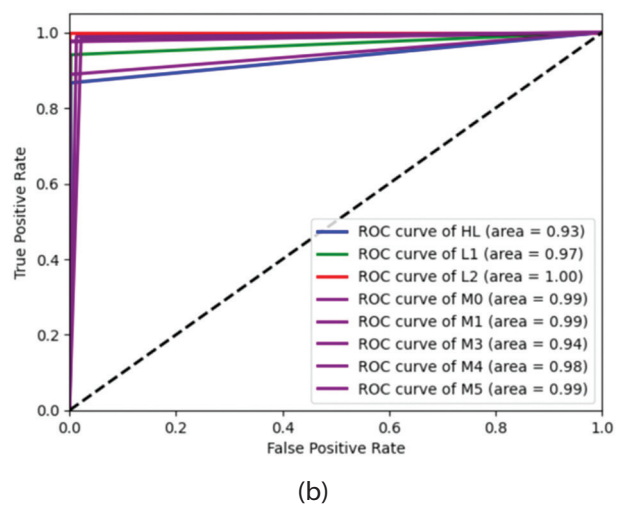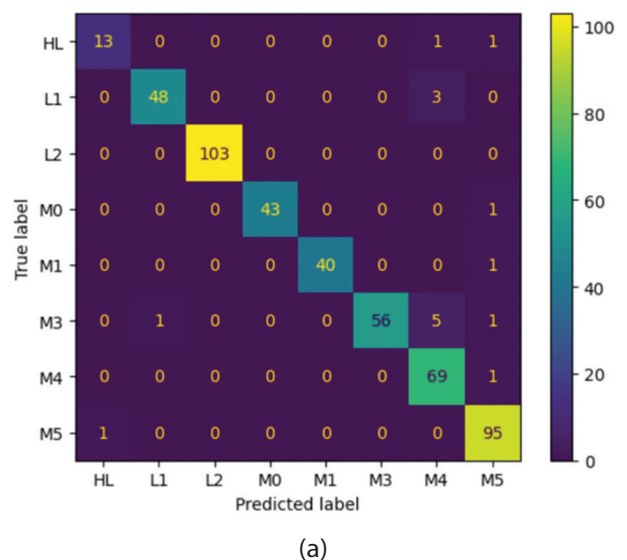
Fig. 5. (**a**) Confusion Matrix;
(**b**) ROC Curve of classification output
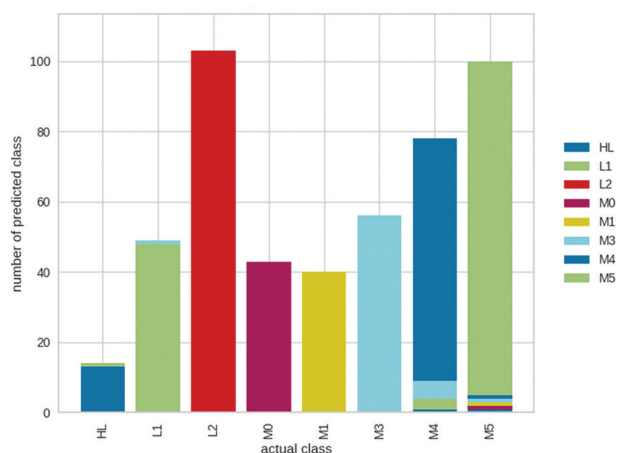
Fig. 6. Class Prediction Error Chart

Fig. 6 illustrates the class prediction error for the classifier. Each bar within the chart depicts the proportion of predictions for individual classes, offering a rapid comprehension of the classifier's accuracy in assigning correct classes. This model demonstrates proficient prediction for L2, M0, M1, and M3 subtypes based on

the feature vector. However, it exhibits some inaccuracies in predicting HL, L1, M4, and M5 types.

6. CONCLUSION

Acute leukemia is rapid progression disease that leads to generation of white blood cells which are abnormal and can potentially spread to other organs, causing health issues. Timely diagnosis and treatment are essential for effective management. This paper suggests an automated machine learning approach for the early detection of acute leukemia, as well as its classification into the two primary types, ALL and AML. Furthermore, it aims to categorize these types into their respective subtypes, which include L1, L2, M0, M1, M3, M4, and M5. The suggested model comprises three key phases. The initial phase involves Segmentation and Nucleus Cropping, which encompasses extracting the green channel from the original image and converting it to the YCbCr color space. A Median filter is then applied to eliminate any noise, creating a nucleus mask through watershed segmentation, and ultimately cropping the nucleus using a bounding box. The second phase focuses on Feature Extraction, encompassing the extraction of various features, such as texture, geometric, color, and statistical attributes, from the region of interest. The final phase involves Classification, employing a Random Forest classifier to categorize the samples into ALL, AML, ALL Subtypes, AML Subtypes, and healthy cells. With an impressive accuracy rate of 97% and hamming loss of 0.03%, this model has the potential to significantly assist pathologists and medical professionals in swiftly identifying cases of Acute Leukemic cancer, thereby facilitating prompt decision-making for accurate diagnoses. Furthermore, there is room for further enhancements and refinements in the methodology to potentially raise the classification accuracy even higher, ultimately improving the model's utility in clinical settings.

7. REFERENCES:

[1] Leukaemia, https://gco.iarc.fr/today/data/fact-sheets/cancers/36-Leukaemia-fact-sheet.pdf (accessed: 2023)

[2] D. A. Arber, A. Orazi, R. Hasserjian, J. Thiele, M. J. Borowitz, M. M. Le Beau, C. D. Bloomfield, M. Cazzola, J. W. Vardiman, "The 2016 revision to the World Health Organization classification of myeloid neoplasms and acute leukemia", Blood, Vol. 127, No. 20, 2016, pp. 2391-405.

[3] S. Shimony, M. Stahl, R. Stone, "Acute myeloid leukemia: 2023 update on diagnosis, risk-stratification, and management", American Journal of Hematology, Vol. 98, No. 3, 2023, pp. 502–526.

[4] K. Gupta, N. Jiwani, P. Whig, "Effectiveness of Machine Learning in Detecting Early-Stage Leukemia", Proceedings of the International Conference on Innovative Computing and Communications, Delhi, India, 19-20 February 2022, pp. 461-472.

[5] L. Putzu, G. Caocci, C. Di Ruberto, "Leucocyte classification for leukaemia detection using image processing techniques", Artificial Intelligence in Medicine, Vol. 62, No. 3, 2014, pp. 179-191.

[6] S. Mohapatra, D. Patra, S. Satpathy, "An ensemble classifier system for early diagnosis of acute lymphoblastic leukemia in blood microscopic images", Neural Computing and Applications, Vol. 24, 2014, pp. 1887-1904.

[7] J. Rawat, A. Singh, B. Hs, J. Virmani, J. S. Devgun, "Computer assisted classification framework for prediction of acute lymphoblastic and acute myeloblastic leukemia", Biocybernetics and Biomedical Engineering, Vol. 37, No. 4, 2017, pp. 637-654.

[8] H. H. Inbarani, A. T. Azar, G. Jothi, "Leukemia image segmentation using a hybrid Histogram-Based soft covering rough K-Means clustering algorithm", Electronics, Vol. 9, No. 1, 2020, p. 188.

[9] T. G. Devi, N. Patil, S. Rai, C. S. Philipose, "Gaussian Blurring Technique for Detecting and Classifying Acute Lymphoblastic Leukemia Cancer Cells from Microscopic Biopsy Images", Life, Vol. 13, 2023, p. 348.

[10] M. Ashok, K. Tharani, S. VenkataSriram, K. Ramasamy, "An Investigational Study of Detecting Acute Lymphoblastic Leukemia using Computer Vision", Proceedings of the 2nd International Conference on Smart Technologies and Systems for Next Generation Computing, Villupuram, India, 21-22 April 2023, pp. 1-6.

[11] P. K. Das, D. V. A, S. Meher, R. Panda, A. Abraham, "A Systematic Review on Recent Advancements in Deep and Machine Learning Based Detection and Classification of Acute Lymphoblastic Leukemia", IEEE Access, Vol. 10, 2022, pp. 81741-81763.

[12] R. Raina et al. "A Systematic Review on Acute Leukemia Detection Using Deep Learning Techniques", Archives of Computational Methods in Engineering, Vol. 30, 2023, pp. 251-270.

[13] S. Ansari, A. H. Navin, A. B. Sangar, J. V. Gharamaleki, S. Daneshvar, "A customized efficient deep learning model for the diagnosis of acute leukemia cells based on lymphocyte and monocyte images", Electronics, Vol. 12, No. 2, 2023, p. 322.

[14] L. Boldú, A. Merino, A. Acevedo, A. Molina, J. Rodellar, "A deep learning model (ALNet) for the diagnosis of acute leukaemia lineage using peripheral blood cell images", Computer Methods and Programs in Biomedicine, Vol. 202, 2021.

[15] S. M. Abass, A. M. Abdulazeez, D. Q. Zeebaree, "A YOLO and convolutional neural network for the detection and classification of leukocytes in leukemia", Indonesian Journal of Electrical Engineering and Computer Science, Vol. 25, No. 1, 2022, pp. 200-213.

[16] S. Saleem, J. Amin, M. Sharif, G. A. Mallah, S. Kadry, A. H. Gandomi, "Leukemia segmentation and classification: A comprehensive survey", Computers in Biology and Medicine, Vol. 150, 2022, p. 106028.

[17] P. Manescu et al. "Detection of acute promyelocytic leukemia in peripheral blood and bone marrow with annotation-free deep learning", Scientific Reports, Vol. 13, 2023, p. 2562.

[18] D. S. Depto, Md. M. Rizvee, A. Rahman, H. Zunair, M. S. Rahman, M. R. C. Mahdy, "Quantifying imbalanced classification methods for leukemia detection", Computers in Biology and Medicine, Vol. 152, 2023, p. 106372.

[19] W. H. Abir, M. F. Uddin, F. R. Khanam, T. Tazin, M. M. Khan, M. Masud, S. Aljahdali, "Explainable AI in Diagnosing and Anticipating leukemia using transfer Learning Method", Computational Intelligence and Neuroscience, Vol. 2022, 2022, pp. 1-14.

[20] T. A. M. Elhassan, M. S. M. Rahim, T. T. Swee, S. Z. M. Hashim, M. Aljurf, "Feature Extraction of White Blood Cells Using CMYK-Moment Localization and Deep Learning in Acute Myeloid Leukemia Blood Smear Microscopic Images", IEEE Access, Vol. 10, 2022, pp. 16577-16591.

[21] K. K. Jha, H. S. Dutta, "Mutual Information based hybrid model and deep learning for Acute Lymphocytic Leukemia detection in single cell blood smear images", Computer Methods and Programs in Biomedicine, Vol. 179, 2019, p. 104987.

[22] Z. M. Kouzehkanan et al. "A large dataset of white blood cells containing cell locations and types, along with segmented nuclei and cytoplasm", Scientific Reports, Vol. 12, No. 1, 2022, p. 1123.